Interaction-induced time-symmetry breaking in driven quantum oscillators

M. I. Dykman, Christoph Bruder, Niels Lörch, and Yaxing Zhang

Phys. Rev. B **98**, 195444 — Published 29 November 2018

DOI: 10.1103/PhysRevB.98.195444

Interaction-induced time-symmetry breaking in driven quantum oscillators

M. I. Dykman,[1] Christoph Bruder,[2] Niels Lörch,[2] and Yaxing Zhang[3]

[1] *Department of Physics and Astronomy, Michigan State University, East Lansing, Michigan 48824, USA*
[2] *Department of Physics, University of Basel, Klingelbergstrasse 82, CH-4056 Basel, Switzerland*
[3] *Department of Physics, Yale University, New Haven, Connecticut 06511, USA*

(Dated: November 11, 2018)

We study parametrically driven quantum oscillators and show that, even for weak coupling between the oscillators, they can exhibit various many-body states with broken time-translation symmetry. In the quantum-coherent regime, the symmetry breaking occurs via a nonequilibrium quantum phase transition. For dissipative oscillators, the main effect of the weak coupling is to make the switching rate of an oscillator between its period-2 states dependent on the states of other oscillators. This allows mapping the oscillators onto a system of coupled spins. For identical oscillators, the stationary state can be mapped on that of the Ising model with an effective temperature $\propto \hbar$, for low temperature. If the oscillators are different and are away from the bifurcation parameter values where the period-2 states emerge, the stationary state corresponds to having a microscopic current in the spin system. Close to the bifurcation point the coupling can not be considered weak and the system maps onto coupled overdamped Brownian particles performing quantum diffusion in a potential landscape.

I. INTRODUCTION

Time-symmetry breaking in periodically modulated quantum systems, often called a "time crystal" effect[1], has been attracting much attention recently. One of the most challenging problems in this rapidly developing area is the understanding of the interplay of interaction, disorder, and dissipation[2–9]. In particular, disorder helps preventing heating of the system by a periodic drive in the coherent regime[10–12]. However, the dependence of the lifetime of the broken-symmetry state on the disorder strength is not known generally and is likely to be model-dependent. Disorder should not be necessary in the presence of dissipation. An example is the observation of an interaction-induced breaking of the time-translation symmetry in a dissipative classical cold-atom system[13]. A microscopic theory mapped the effect onto a phase transition in an all-to-all coupled Ising system, and the measured critical exponents were in agreement with this mapping[14].

Closely related to the problem of time-symmetry breaking is *computing* with parametric oscillators[15–22]. A weakly nonlinear classical dissipative oscillator displays period doubling when its eigenfrequency ω_0 is modulated at a frequency ω_F close to $2\omega_0$[23]. The emerging period-2 states have opposite phases, see Fig. 1. They can be associated with two states of a classical bit[24], or two spin states. The spin analogy was studied in recent numerical work for up to four coupled quantum parametric oscillators and, for a number of parameter values, it was shown that the system can be mapped onto an "Ising machine" in the coherent[19] as well as the dissipative regime[20–22]. If the system is in one of the period-2 states, time-translation symmetry is broken, since the period of the motion is $4\pi/\omega_F \approx 2\pi/\omega_0$ instead of $2\pi/\omega_F$.

In this paper we study the possibility and the nature of time-symmetry breaking in a large system of coupled quantum parametric oscillators. Of interest to us are the broken-symmetry phases that emerge both in the coherent and in the dissipative regimes. Our formulation applies in the presence of weak disorder.

The relevant physical systems are microwave modes in superconducting cavities that can be coupled into lattices with variable geometry[25–27], as well as coupled vibrational modes in networks of nanomechanical resonators[18,28,29]. An advantageous feature of these systems is the possibility to make them one- or two-dimensional, control the coupling strength, and implement various coupling geometries which, at least in the nanomechanical setting, are not limited to nearest-neighbor coupling. We assume the coupling of the modes in different resonators to be comparatively weak and the mode eigenfrequencies to form a narrow band centered at a characteristic eigenfrequency ω_0. In the absence of a periodic drive, the spectrum of excitations is therefore also a narrow band centered near ω_0.

The effect of the coupling is significantly more complicated for parametrically excited modes (oscillators). To understand it, we note first that the quantum dynamics of an isolated oscillator can be mapped onto the dynamics of an auxiliary particle with a double-well quasienergy Hamiltonian[30]. The Hamiltonian is symmetric; the two minima correspond to the opposite phases of the period-2 oscillations, see Fig. 1. The oscillator can tunnel between the minima, which leads to phase-flip transitions. However, if the relaxation rate largely exceeds the tunnel splitting, the interwell switching occurs via effectively "overbarrier" transitions. This happens even for $T = 0$ due to the quantum noise which invariably accompanies relaxation[30]. One can associate the minima of the Hamiltonian of the $\varkappa$th oscillator with a spin $\sigma_\varkappa = \pm 1$. The switching rates $W_{\sigma_\varkappa} \equiv W_{\sigma_\varkappa \to -\sigma_\varkappa}$ between the minima are equal by symmetry.

If the oscillators are coupled and one of them is in a certain state (near one of the minima of the quasienergy Hamiltonian, see Fig. 1), the symmetry of the effective

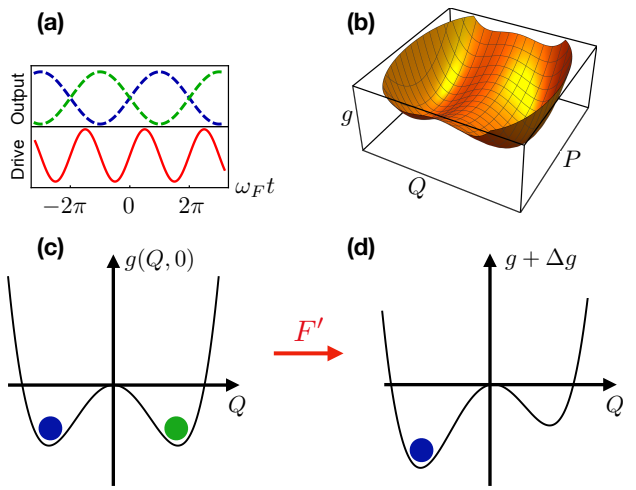

FIG. 1. (a) Period doubling of a weakly nonlinear classical dissipative oscillator parametrically driven at a frequency ω_F that is close to twice the oscillator eigenfrequency ω_0. (b) The scaled Hamiltonian g of the oscillator as a function of the scaled coordinate Q and momentum P in the frame rotating at frequency $\omega_F/2$ in the rotating wave approximation. (c) Cut $g(Q,0)$ through (b) at $P=0$. The blue (left) and green (right) circles indicate the stable positions of the oscillator in the rotating frame, which correspond to the oscillations in the lab frame shown by the blue and green dashed lines in (a). (d) If the oscillator is additionally driven by a field F' at frequency $\omega_F/2$, the extra term Δg in the oscillator Hamiltonian breaks the symmetry. As we show, a similar effect results from the coupling of parametric oscillators.

Hamiltonian for the oscillator coupled to it is broken. Then, for this oscillator, the switching rates between the minima become different. Depending on the sign of the coupling, the "deeper" well corresponds to the oscillators having the same (for the case of attractive coupling) or the opposite (for the case of repulsive coupling) phase.

It is important that the rates $W_{\sigma_\varkappa}$ are much smaller than the inverse t_r^{-1} of the relaxation time. Therefore, when one of the oscillators is switching, the oscillators coupled to it are most likely localized in a certain minimum. As we show, the change of the switching rate $W_{\sigma_\varkappa}$ of oscillator $\varkappa$ due to its coupling to oscillators $\varkappa'$ can be large even for weak coupling, with $\log W_{\sigma_\varkappa}$ being linear in the coupling. This allows one to map the problem onto the Ising model of coupled spins, for identical oscillators.

The well-known properties of the Ising model imply that, for not too weak attractive coupling, the most probable state of the many-mode two-dimensional system is the broken-symmetry state with all $\sigma_\varkappa$ equal, i.e., the phases of all oscillators being the same. In this state, the symmetry with respect to time translation by the drive period is broken. For the case of repulsive mode coupling, the system of coupled modes maps onto the antiferromagnetically coupled Ising model and can exhibit frustration, depending on the geometry of the lattice and the structure of the coupling.

We emphasize that the occurrence of the Ising-type regime is a consequence of the coupling of the oscillators. If the oscillators are uncoupled (or if the coupling is very weak), the distribution over the two phases of parametrically excited vibrations is uniform and the system as a whole does not display time-symmetry breaking.

If the oscillators are close to the bifurcation point where period-two states emerge, their coupling becomes effectively stronger, and the appropriate picture is that of a multiple-well "quasienergy landscape". This landscape has global symmetry with respect to time translation $t \to t + 2\pi/\omega_F$, but each individual minimum does not have this symmetry. As a result, in the presence of disorder there may be many metastable broken-symmetry states. Quantum noise leads to diffusion between these states, but the transitions between different minima involve many modes and become exponentially slow. The system effectively "freezes" in one of them, and time-translation symmetry is then broken.

In the quantum-coherent regime, a new phenomenon appears: instead of a bifurcation point for each individual oscillator, the coupled modes exhibit a nonequilibrium quantum phase transition (QPT). The control parameter is the distance to the critical value of the drive frequency $\omega_F = \omega_{\rm QPT}$, or to the critical value of the drive amplitude. We will consider the case where there is no disorder and the oscillators are on a lattice. The spectrum of excitations of the system can be naturally defined, if one starts from the symmetric state (below the QPT), where the oscillators are not excited and all of them occupy the ground state. Here the spectrum is gapped, see Fig. 2 (in the absence of driving, it is just the spectrum of optical phonons in a crystal). It is convenient to picture the spectrum by downshifting the excitation frequency by $\omega_F/2$. Then the spectral gap goes to zero at the phase transition point and the dispersion law of the long-wavelength excitations becomes linear. For attractive coupling between the oscillators, beyond the QPT the system has a state where all of them vibrate in phase and the excitation spectrum is again gapped. This state has broken time-translation symmetry, a direct analog of the ferromagnetic state of an Ising chain that goes through a QPT on varying the transverse magnetic field[31,32].

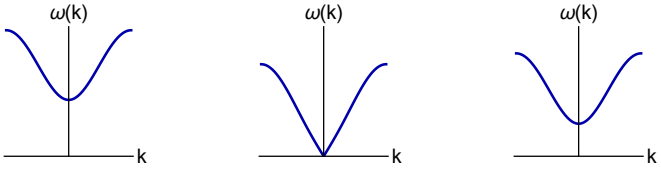

FIG. 2. Sketch of the excitation spectrum $\omega(k)$ near the quantum phase transition in the frame rotating at $\omega_F/2$. If the control parameter μ is below (left panel) or above (right panel) the critical value $\mu_{\rm QPT}$, the spectrum is gapped. For $\mu = \mu_{\rm QPT}$, the spectrum becomes linear for $k \to 0$.

The paper is organized as follows: In Sec. II below we describe the Hamiltonian of the system. In Sec. III we

show how the problem of weakly coupled parametric oscillators can be described in terms of an exponentially strong modification of the rate of interstate switching of an oscillator depending on the state of other oscillators. The description is based on the notion of the logarithmic susceptibility. It allows mapping the system onto an Ising system provided there is detailed balance. This is the case if the oscillators are identical. Using results of a calculation of the logarithmic susceptibility sketched in Appendix A, Sec. IV analyzes coupled oscillators near the threshold of parametric excitation. One of its results is a spin-glass type phase where the system can have many metastable states with broken time-translation symmetry. Section V describes a quantum time-symmetry breaking transition in a spatially-periodic system of coupled oscillators. Section VI summarizes the results and contains concluding remarks.

II. THE MODEL

We consider a system of coupled quantum oscillators (modes). They are weakly nonlinear and are parametrically modulated. The Hamiltonian of the system is

$$H = H_0 + H_F + H_c\,, \tag{1}$$

where

$$H_0 = \frac{1}{2}\sum_{\varkappa}(p_\varkappa^2 + \omega_\varkappa^2 q_\varkappa^2) + \frac{1}{4}\gamma\sum_{\varkappa} q_\varkappa^4\,. \tag{2}$$

Here, $\varkappa = 1, 2, \ldots, N$ enumerates the oscillators, $q_\varkappa$ and $p_\varkappa$ are their coordinates and momenta, and $\omega_\varkappa$ are their eigenfrequencies; we assume that the values of $\omega_\varkappa$ are close to each other, $|\omega_\varkappa - \omega_0| \ll \omega_0$. The parameter γ characterizes the lowest-order nonlinearity that is relevant for resonantly excited small-amplitude oscillations[23]. In what follows we assume $\gamma > 0$; an extension to the case $\gamma < 0$ is straightforward.

The Hamiltonian H_F describes resonant parametric driving,

$$H_F = \frac{1}{2}\sum_{\varkappa} q_\varkappa^2 F\cos\omega_F t, \quad \omega_F \approx 2\omega_0\,, \tag{3}$$

and H_c is the Hamiltonian of the coupling between the modes,

$$H_c = -\frac{1}{2}\sum_{\varkappa\neq\varkappa'}\varepsilon_{\varkappa\varkappa'} q_\varkappa q_{\varkappa'}\,, \quad |\varepsilon_{\varkappa\varkappa'}| \ll \omega_0^2\,. \tag{4}$$

This coupling corresponds to a bilinear mode interaction and occurs, e.g., in microwave cavity arrays and in systems of mechanical nanoresonators[26,28,29]. The oscillator nonlinearity, the coupling, and the driving are assumed to be weak, $\gamma\langle q_\varkappa^2\rangle, |\varepsilon_{\varkappa\varkappa'}|, |F| \ll \omega_0^2$. In this case the motion of the oscillators corresponds to vibrations at frequency $\approx \omega_F/2$ with amplitude and phase that slowly vary on the time scale $1/\omega_F$. This motion can be conveniently described in the rotating frame by introducing the ladder operators $a_\varkappa, a_\varkappa^\dagger$ of the $\varkappa$th oscillator, applying a canonical transformation $U(t) = \exp[-i(\omega_F t/2)\sum_\varkappa a_\varkappa^\dagger a_\varkappa]$ and switching to the scaled coordinates $Q_\varkappa$ and momenta $P_\varkappa$ that slowly vary in time,

$$U^\dagger(t)[q_\varkappa + (2i/\omega_F)p_\varkappa]U(t) = -iC(Q_\varkappa + iP_\varkappa)e^{-i\omega_F t/2},$$
$$[P_\varkappa, Q_{\varkappa'}] = -i\lambda\delta_{\varkappa\varkappa'}, \qquad \lambda = 3\hbar\gamma/\omega_F F. \tag{5}$$

Here, we chose $F > 0$ and set $C = (2F/3\gamma)^{1/2} = (2\hbar/\lambda\omega_F)^{1/2}$; in Appendix B we use a different scaling to describe the quantum phase transition induced by the varying field amplitude. The parameter λ is the dimensionless Planck constant in the rotating frame; we note that, in terms of the scaled variables $Q_\varkappa, P_\varkappa$, the lowering operator is $a_\varkappa = (2\lambda)^{-1/2}(Q_\varkappa + iP_\varkappa)$.

We assume that the scaled Planck constant is small, $\lambda \ll 1$. This means that the dynamics in the rotating frame is semiclassical and the states of parametrically excited period-2 oscillations of the individual mode overlap only weakly.

A. The rotating wave approximation

For weak nonlinearity and weak mode coupling, the resonant dynamics of the coupled modes can be conveniently described in the rotating wave approximation (RWA). In this approximation the canonically transformed Hamiltonian of the system becomes

$$U^\dagger H U - i\hbar U^\dagger\dot{U} \approx (3\gamma C^4/8)\mathbb{G}\,,$$
$$\mathbb{G} = \sum_{\varkappa} g_\varkappa(Q_\varkappa, P_\varkappa) + g_c\,. \tag{6}$$

Here, $\mathbb{G}$ is the scaled RWA Hamiltonian of the system. It is the sum of the scaled RWA Hamiltonians $g_\varkappa(Q_\varkappa, P_\varkappa) \equiv g_\varkappa(Q_\varkappa, -i\lambda\partial_{Q_\varkappa})$ of the individual oscillators and the coupling term g_c. The individual Hamiltonians $g_\varkappa$ depend on a single parameter $\mu_\varkappa$ and can be expressed as[30]

$$g_\varkappa(Q_\varkappa, P_\varkappa) = \frac{1}{4}(P_\varkappa^2 + Q_\varkappa^2 - \mu_\varkappa)^2 + \frac{1}{2}(P_\varkappa^2 - Q_\varkappa^2) - \frac{\mu_\varkappa^2}{4}\,,$$
$$\mu_\varkappa = 2\delta\omega_\varkappa\omega_F/F, \qquad \delta\omega_\varkappa = \frac{1}{2}\omega_F - \omega_\varkappa\,. \tag{7}$$

The parameter $\mu_\varkappa$ is determined by the ratio of two small parameters, the detuning $\delta\omega_\varkappa$ of half the drive frequency from the mode eigenfrequency and the scaled drive amplitude F/ω_F. For $\mu_\varkappa < -1$, $g_\varkappa(Q_\varkappa, P_\varkappa)$ has a single minimum at $Q_\varkappa = P_\varkappa = 0$. This minimum corresponds to the equilibrium position of the oscillator in the laboratory frame. As $\mu_\varkappa$ increases beyond -1, the point $Q_\varkappa = P_\varkappa = 0$ becomes first a saddle point, and then, for $\mu_\varkappa > 1$, a local maximum of $g_\varkappa$. In addition, for $\mu_\varkappa > -1$, the function $g_\varkappa$ has two symmetrically located minima at $P_\varkappa = 0, Q_\varkappa = \pm(\mu_\varkappa+1)^{1/2}$. They can be seen

in Fig. 1. Classically, in the presence of weak dissipation these minima become stable states. They correspond to two states of period-2 oscillations with opposite phases. We enumerate them by

$$\sigma_\varkappa = \pm 1;$$

for concreteness, we set $\sigma_\varkappa = 1$ to correspond to the minimum of $g_\varkappa$ with $Q_\varkappa > 0$.

The term g_c in Eq. (6) describes the coupling Hamiltonian in the rotating frame,

$$g_c = -\frac{1}{2}\sum_{\varkappa\neq\varkappa'} V_{\varkappa\varkappa'}(Q_\varkappa Q_{\varkappa'} + P_\varkappa P_{\varkappa'}) ,$$
$$V_{\varkappa\varkappa'} = 2\varepsilon_{\varkappa\varkappa'}/F . \qquad (8)$$

We note that the coupling in the coordinate channel in the lab frame described by Eq. (4) becomes symmetric with respect to the coordinates and momenta in the rotating frame, in the RWA.

The effect of the coupling on the mode dynamics depends on the relation between $|V_{\varkappa\varkappa'}|$ and the depth of the wells of the functions $g_\varkappa$, see Fig. 1. If $|V_{\varkappa\varkappa'}|$ is small, the overall many-mode Hamiltonian (6) is a set of double-well functions $g_\varkappa$ slightly distorted by the coupling. If, on the other hand, the coupling is comparatively strong, the overall structure of the Hamiltonian changes. We will not consider this case in the present paper.

Corrections to the rotating wave approximation vanish like $(\delta\omega_\varkappa/\omega_F)^2, (V_{\varkappa\varkappa'}/\omega_F)^2$. They do not break the underlying symmetry discussed in Sec. II A 1. In the special case where the spacing between the intrawell and over-the-barrier quasienergies coincides with a multiple of $\hbar\omega_F$ these corrections may modify the tunneling of an isolated oscillator between its coexisting stable states[33]. However, interwell tunneling is irrelevant in the context of the present paper: it is exponentially suppressed in the system of coupled oscillators. Here and below we refer to quasienergies in the extended Brillouin zone, i.e., not projected onto a single interval of width $\hbar\omega_F$. The values of the quasienergies of an isolated oscillator are given by the eigenvalues of operator $g_\varkappa$ multiplied by $F^2/6\gamma$ (except for the corrections to the RWA mentioned above).

1. Symmetry arguments

The RWA Hamiltonian $\mathbb{G}$ has inversion symmetry, both with respect to the simultaneous sign change of all coordinates, $\{Q_\varkappa \to -Q_\varkappa\}$, or all momenta, $\{P_\varkappa \to -P_\varkappa\}$. This symmetry is a consequence of the parity of the Hamiltonian H in $\{p_\varkappa\}$ and the symmetry of H with respect to time translation by the driving period $t \to t + 2\pi/\omega_F$. From Eq. (5), such a translation corresponds to changing the signs of $\{Q_\varkappa, P_\varkappa\}$. Indeed, as a result of the time translation, the unitary operator $U(t)$ in Eq. (5) becomes $U(t + 2\pi/\omega_F) = U(t)N_2$, where $N_2 = \exp(-i\pi\sum_\varkappa a_\varkappa^\dagger a_\varkappa)$. The time-translation operator N_2 flips the sign of the mode coordinates and momenta, $N_2^\dagger q_\varkappa N_2 = -q_\varkappa$ and similarly for $p_\varkappa$. In addition, N_2 commutes with $\mathbb{G}$. Therefore, as in the case of a single oscillator[34,35], the eigenfunctions of $\mathbb{G}$ are the Floquet eigenfunctions of the original time-periodic Hamiltonian H. The eigenvalues of $\mathbb{G}$ are the RWA-quasienergies of the system scaled by the factor $F^2/6\gamma$.

The individual RWA Hamiltonians $g_\varkappa$ also have inversion symmetry, cf. Fig. 1. Therefore, generally, the intrawell states of $g_\varkappa$ are tunnel-split into symmetric and antisymmetric states. For a small dimensionless Planck constant λ, this splitting is small deep inside the wells and may be equal to zero for certain $\mu_\varkappa$[36].

B. Quantum kinetic equation

We now discuss the dissipative dynamics of the system of parametric oscillators. To this end, we will assume that each oscillator is coupled to its own thermal reservoir and that all reservoirs have the same temperature. We will use the simplest model where the interaction with the reservoirs is linear in $q_\varkappa, p_\varkappa$. If the densities of states of the reservoirs weighted with the coupling to the oscillators are sufficiently smooth near ω_0, the oscillators dynamics in "slow time"

$$\tau \equiv tF/2\omega_F \qquad (9)$$

is Markovian. A derivation is a straightforward extension of the derivation for a single nonlinear oscillator[37] to the case of coupled oscillators; the frequency renormalization is incorporated into $\omega_\varkappa$. For simplicity, we will assume that the decay rates of all the oscillators are the same: different decay rates constitute a dissipative type of disorder and will not be discussed in this paper.

With these assumptions, the master equation for the multi-oscillator density matrix ρ reads

$$\dot\rho \equiv \frac{d\rho}{d\tau} = \frac{i}{\lambda}[\rho, \mathbb{G}] + \kappa\sum_\varkappa \mathcal{D}[a_\varkappa]\rho ,$$
$$\mathcal{D}[a]\rho = -(\bar n + 1)\left(a^\dagger a\rho - 2a\rho a^\dagger + \rho a^\dagger a\right)$$
$$-\bar n\left(aa^\dagger\rho - 2a^\dagger\rho a + \rho aa^\dagger\right) . \qquad (10)$$

Here, κ is the dimensionless oscillator decay rate; it is related to the decay rate Γ of free vibrations amplitude in unscaled time as $\kappa = 2\Gamma\omega_F/F$. Parameter $\bar n = [\exp(\hbar\omega_F/2k_BT) - 1]^{-1}$ is the oscillator Planck number.

Alternatively, and this will be used below, one can write down the quantum Langevin equations

$$\dot Q_\varkappa = -\kappa Q_\varkappa + \partial_{P_\varkappa}\mathbb{G} + f_{Q_\varkappa}(\tau) ,$$
$$\dot P_\varkappa = -\kappa P_\varkappa - \partial_{Q_\varkappa}\mathbb{G} + f_{P_\varkappa}(\tau) . \qquad (11)$$

Here, $f_{Q_\varkappa}(\tau)$ and $f_{P_\varkappa}(\tau)$ are δ-correlated operators,

$$\langle f_{Q_\varkappa}(\tau)f_{Q_{\varkappa'}}(\tau')\rangle = \langle f_{P_\varkappa}(\tau)f_{P_{\varkappa'}}(\tau')\rangle$$
$$= 2D\delta(\tau - \tau')\delta_{\varkappa\varkappa'}, \qquad D = \frac{1}{2}\lambda\kappa(2\bar n + 1) , \qquad (12)$$

and $\langle [f_{Q_\varkappa}(\tau), f_{P_{\varkappa'}}(\tau')]\rangle = 2i\lambda\kappa\delta(\tau-\tau')\delta_{\varkappa\varkappa'}$. For small λ the noise intensity D is small. Equation (11) is the Heisenberg version of the master equation (10). The partial derivatives of $\mathbb{G}$ in Eq. (11) should be interpreted as symmetrized expressions, for example, $\partial_P(P^2+Q^2)^2 = 2P(P^2+Q^2)+2(P^2+Q^2)P$.

1. The equilibrium positions of an isolated oscillator

For an isolated parametrically excited oscillator $\varkappa$, in the absence of noise, Eqs. (11) have stable stationary solutions $(\sigma_\varkappa Q_\varkappa^{(0)}, \sigma_\varkappa P_\varkappa^{(0)})$ given by

$$
\begin{aligned}
&Q_\varkappa^{(0)} = (\mu_\varkappa - \mu_B)^{1/2}\cos\Phi_\varkappa, \qquad \Phi_\varkappa = \arctan\frac{\kappa}{1-\mu_B},\\
&P_\varkappa^{(0)} = (\mu_\varkappa - \mu_B)^{1/2}\sin\Phi_\varkappa\,,\\
&\mu_B = -(1-\kappa^2)^{1/2}
\end{aligned}
\tag{13}
$$

Here, $\sigma_\varkappa = \pm 1$ enumerates the vibrational states with opposite phase. As before, we set $\sigma_\varkappa = 1$ for the state with positive $Q_\varkappa^{(0)}$.

The coefficient μ_B in Eq. (13) is the value of $\mu_\varkappa$ at the bifurcation where the zero-amplitude state $Q_\varkappa = P_\varkappa = 0$ becomes dynamically unstable and the two stable period-2 states emerge. In the model we use here, where the decay rate in the scaled time is the same for all modes, μ_B is also the same for all modes. In this paper we concentrate on the parameter range $\mu_\varkappa < -\mu_B$, where an isolated oscillator has either two stable period-2 states (for $\mu_\varkappa > \mu_B$) or a stable zero-amplitude state (for $\mu_\varkappa < \mu_B$), but not the case where all these states are stable.

In the Wigner representation, the probability distribution $\rho_\varkappa(Q_\varkappa, P_\varkappa)$ of an isolated oscillator has peaks which are centered near $(\sigma_\varkappa Q_\varkappa^{(0)}, \sigma_\varkappa P_\varkappa^{(0)})$. For weak damping, the positions of the peaks are close to the minima of $g_\varkappa(Q_\varkappa, P_\varkappa)$, cf. Fig. 1, and the width of the peaks is $\sim \lambda^{1/2}$ for $\bar{n} \lesssim 1$[30,38]. However, the peaks can be well-resolved even if the broadening $\kappa\lambda$ of the quasienergy levels (which, we remind, are given by the scaled eigenvalues of $g_\varkappa$) is not small compared to the interlevel distance. The distribution is symmetric, $\rho_\varkappa(Q_\varkappa, P_\varkappa) = \rho_\varkappa(-Q_\varkappa, -P_\varkappa)$.

III. TIME-SYMMETRY BREAKING FOR WEAKLY COUPLED OSCILLATORS

In this section we show that even weak mode coupling can lead to a collective breaking of the time-translation symmetry of dissipative oscillators if the quantum noise is sufficiently weak. The underlying mechanism is the coupling-induced change of the rate of switching between the period-2 states of the oscillators. It should be emphasized that the time-symmetry breaking for the driven oscillator corresponds to the breaking of the symmetry of the system described by the stationary Hamiltonian $\mathbb{G}$ in phase space. Therefore the results[39] on the absence of time-symmetry breaking in a stationary system in the ground state do not apply to our case. Rather, the symmetry breaking for the time-independent Hamiltonian $\mathbb{G}$ resembles the symmetry breaking in an Ising system. In the lab frame, though, it corresponds to the breaking of the discrete time-translation symmetry.

The dissipative dynamics of an isolated parametric oscillator $\varkappa$ is characterized by the dimensionless relaxation rate κ and by the switching rate $W_{\sigma_\varkappa}$ from the well $\sigma_\varkappa$ to the well $-\sigma_\varkappa$ of the RWA Hamiltonian $g_\varkappa$. To simplify notations, here and below we use $W_{\sigma_\varkappa}$ for the dimensionless switching rate and imply the dimensionless time τ when discussing time evolution. The dimensionless switching rates are exponentially smaller than the relaxation rate, $W_{\sigma_\varkappa} \ll \kappa$. The oscillator approaches one of the minima of $g_\varkappa$ on a time scale $\sim \kappa^{-1}$. It performs quantum fluctuations about this minimum for a time much longer than κ^{-1}, until ultimately it switches to the other minimum.

If κ largely exceeds the exponentially small tunnel splitting of the intrawell states, the interwell switching occurs via "overbarrier" transitions[30]. Such transitions result from quantum diffusion over the intrawell quasienergy states, which brings the system from the bottom of the initially occupied well of $g_\varkappa$ to the top of the interwell barrier. This process is reminiscent of the familiar thermally activated overbarrier transitions in classical systems[40], except that, for low temperatures, it is induced by quantum fluctuations and, respectively, is called quantum activation. The physical cause of the diffusion over quasienergy states is that quantum relaxation is invariably associated with noise. Relaxation results from transitions between the states of the oscillator with emission of excitations of the thermal reservoir, but these transitions happen at random, and therefore they bring in noise. The presence of this quantum noise is reflected in the noise terms in Eq. (11).

For an isolated oscillator $\varkappa$, the rate of switching due to quantum activation has the form

$$W_{\sigma_\varkappa}^{(0)} = \text{const} \times \exp(-R_\varkappa^{(0)}/\lambda).$$

The parameter $R_\varkappa^{(0)}$ is the quantum activation energy. By symmetry, $R_\varkappa^{(0)}$ is the same for switching from the both states $\sigma_\varkappa = \pm 1$. Expressions for $R_\varkappa^{(0)}$ have been found in several important limiting cases[30,38]. Note that in the expression for $W_{\sigma_\varkappa}^{(0)}$ the quantum noise intensity λ plays a role analogous to temperature in the expression for the rate of thermally activated switching. We note that $R_\varkappa^{(0)}$ depends on temperature in terms of the Planck occupation number $\bar{n}$ and for $\bar{n} \gg 1$ we have $R_\varkappa^{(0)} \propto \hbar\omega_\varkappa/T$.

A. Symmetry lifting by an extra field at frequency $\omega_F/2$

Before analyzing the effect of the coupling of the modes, we consider a simpler but directly related problem, viz., the effect of a weak additional field at frequency $\omega_F/2$ on the switching rate. Such a field is described by the term $-F'\sum_{\varkappa} q_{\varkappa}\cos(\varphi_{\varkappa}+\omega_F t/2)$ in the Hamiltonian. It breaks the time-translation symmetry $t \to t+2\pi/\omega_F$. In the rotating frame, the effect of the field $\propto F'$ on the mode dynamics is described by the term

$$\Delta g_{\varkappa}(Q_{\varkappa}, P_{\varkappa}) = -f'(Q_{\varkappa}\sin\varphi_{\varkappa} + P_{\varkappa}\cos\varphi_{\varkappa}) \qquad (14)$$

that has to be added to the RWA Hamiltonian $g_{\varkappa}$, Eq. (7), with $f' = 8F'/3\gamma C^3$.

If the rescaled field f' is small, the term $\Delta g_{\varkappa}$ is small compared to the depth of the wells of $g_{\varkappa}$. However, it can lead to a significant change of the switching rates and, most importantly, make the switching rates $\sigma_{\varkappa} \to -\sigma_{\varkappa}$ different for $\sigma_{\varkappa} = 1$ and $\sigma_{\varkappa} = -1$. In the stationary state, this will lead to a difference of the well populations. In the classical regime, where the interstate switching is thermally activated, the change was discussed previously[41]. We will show in the following section and in Appendix A that, in the quantum regime, too, in several cases of interest the major effect of the drive is to change the quantum activation energy compared to its value $R_{\varkappa}^{(0)}$ in the absence of the drive. The switching rate $W_{\sigma_{\varkappa}}$ then has the form

$$W_{\sigma_{\varkappa}} \propto \exp[-R_{\sigma_{\varkappa}}/\lambda]\,, \qquad R_{\sigma_{\varkappa}} = R_{\varkappa}^{(0)} + \Delta R_{\sigma_{\varkappa}}\,,$$
$$\Delta R_{\sigma_{\varkappa}} = f'\sigma_{\varkappa}(\chi_{Q\varkappa}\sin\varphi_{\varkappa} + \chi_{P\varkappa}\cos\varphi_{\varkappa})\,. \qquad (15)$$

where $R_{\sigma_{\varkappa}}$ is the activation energy for the oscillator $\varkappa$ to switch from the state $\sigma_{\varkappa}$ and $\Delta R_{\sigma_{\varkappa}}$ is its driving-induced part.

In analogy to the classical case, we introduced the logarithmic susceptibilities $\chi_{Q\varkappa}$ and $\chi_{P\varkappa}$ for the variables $Q_{\varkappa}$ and $P_{\varkappa}$ of the mode $\varkappa$. To simplify the further analysis we use a notation that differs from the one used in Ref. 41. To be specific, the susceptibilities $\chi_{Q\varkappa}$ and $\chi_{P\varkappa}$ will be calculated for the well $\sigma_{\varkappa} = 1$. They give the change of the logarithm of the switching rate $W_{\sigma_{\varkappa}}$ linear in the drive f'. The change of the rate can be large even where $|\Delta R_{\sigma_{\varkappa}}| \ll R_{\varkappa}^{(0)}$ provided $|\Delta R_{\sigma_{\varkappa}}| \gg \lambda$. By symmetry, the sign of the change is opposite for the two different wells, and therefore $\Delta R_{\sigma_{\varkappa}} \propto \sigma_{\varkappa}$.

B. Switching rates for coupled modes

The separation of the time scales of relaxation and interwell switching allows one to use the logarithmic susceptibilities to describe the effect of a weak interaction between the oscillators. In the absence of interaction, as seen from the master equation (10), on a time scale long compared to κ^{-1}, the oscillator dynamics can be described as rare uncorrelated switching between the wells. Most of the time each oscillator spends in close vicinity of $\pm(Q_{\varkappa}^{(0)}, P_{\varkappa}^{(0)})$. We emphasize that, in each of these states, the time-translation symmetry is broken.

The major effect of a weak interaction is that, if one oscillator is in a given state $\sigma = \pm 1$, it lifts the time-translation symmetry for the oscillators it is coupled to. In fact, it acts exactly like a driving force $\propto F'$, as it also oscillates at frequency $\omega_F/2$. A symmetry lifting that is similar in spirit was observed for two coupled classical nanomechanical oscillators in the transient process of sweeping the drive frequency ω_F[42].

Put differently, for any given oscillator $\varkappa$, the oscillators $\varkappa'$ with $\varkappa' \neq \varkappa$ act as a drive at frequency $\omega_F/2$. The phase of this drive is determined by the states $\sigma_{\varkappa'}$ of these oscillators. By comparing the expressions for the change of $g_{\varkappa}$ due to an external drive (14) with the expression (8) for the coupling term g_c, we see that the switching rates between the states of the considered oscillator $\varkappa$ have the form

$$W_{\sigma_{\varkappa}} = W_{\sigma_{\varkappa}}^{(0)} \exp\left[-\sigma_{\varkappa}\sum_{\varkappa'}{}' J_{\varkappa\varkappa'}\sigma_{\varkappa'}/\lambda\right],$$
$$J_{\varkappa\varkappa'} = V_{\varkappa\varkappa'}[\chi_{Q\varkappa}Q_{\varkappa'}^{(0)} + \chi_{P\varkappa}P_{\varkappa'}^{(0)}]. \qquad (16)$$

Here we have approximated the dynamical variables $Q_{\varkappa'}, P_{\varkappa'}$ of the oscillators with $\varkappa' \neq \varkappa$ by their most probable values $\sigma_{\varkappa'}Q_{\varkappa'}^{(0)}, \sigma_{\varkappa'}P_{\varkappa'}^{(0)}$.

Equation (16) is the major result of this section. It maps the problem of the coupled parametric oscillators onto a problem of coupled Ising spins. The effect of the spin coupling is to modify the rates of switching between the states of individual spins. The symmetry breaking in this model and its dependence on the dimensionality of the system is well understood. In our case, the effective dimensionality is determined by the connectivity of the oscillator network, for example, the number of nearest neighbors of an oscillator in the network.

An interesting situation occurs if the oscillators slightly differ in frequency or one of the other parameters. In this case the equilibrium positions of different oscillators in the rotating frame $(Q_{\varkappa}, P_{\varkappa})$ are different and so are also the logarithmic susceptibilities. As a result, the spin-coupling parameters are asymmetric, $J_{\varkappa\varkappa'} \neq J_{\varkappa'\varkappa}$. Such a situation is not encountered in the standard analysis of spin systems and is not described by the Ising model discussed below. In the present context it emerges as a consequence of the mapping of a nonequilibrium quantum dissipative system on a system of coupled spins.

C. The stationary distribution. Mapping onto the Ising model

We will now look at the evolution of the distribution $w(\sigma_1, \sigma_2, \ldots)$ of the states $\{\sigma_{\varkappa}\}$ of the system of effective spins. The distribution changes due to switching of the spins, that is, of the individual oscillators, with the rates

given by Eq. (16). Since the switching events are independent, the function w evolves according to the balance equation

$$\dot{w} = -\sum_{\varkappa} W_{\sigma_\varkappa} w(\sigma_1, \ldots, \sigma_\varkappa, \ldots) + \sum_{\varkappa} W_{-\sigma_\varkappa} w(\sigma_1, \ldots, -\sigma_\varkappa, \ldots) \,. \tag{17}$$

The dynamics of the system simplifies in the case of identical oscillators. In this case the susceptibilities $\chi_{Q_\varkappa}, \chi_{P_\varkappa}$ are the same for different oscillators. Then, given that $V_{\varkappa\varkappa'} = V_{\varkappa'\varkappa}$, we have $J_{\varkappa\varkappa'} = J_{\varkappa'\varkappa}$. The coupling parameters $J_{\varkappa\varkappa'}$ are symmetric also if the oscillators are in the vicinity of the bifurcation point, see Sec. IV and Appendix A. Then the stationary solution of Eq. (17) is

$$w_{\rm st} = Z^{-1} \exp\left[-H(\{\sigma_\varkappa\})/\lambda\right] \,, \qquad H(\{\sigma_\varkappa\}) = -\frac{1}{2} \sum_{\varkappa \neq \varkappa'} J_{\varkappa\varkappa'} \sigma_\varkappa \sigma_{\varkappa'} \,. \tag{18}$$

This exactly corresponds to the statistical distribution of an Ising system at effective quantum temperature λ; the normalization constant Z plays the role of the partition function. If the coupling constants of the oscillators $\varepsilon_{\varkappa\varkappa'} \propto V_{\varkappa\varkappa'} \propto J_{\varkappa\varkappa'}$ are positive, the coupling is "ferromagnetic": in the most probable state the values of $\sigma_\varkappa$ are the same for all oscillators, that is, the oscillators vibrate in phase. This is intuitively clear: if the oscillators attract each other, they will try to synchronize into a state where they all vibrate in phase. Whether the system reaches this fully ordered state is determined by the standard results for the ferromagnetic Ising model.

The condition of the phase transition into the symmetry-broken phase is the Ising condition, which for nearest-neighbor coupling in a 2D lattice has the form $J_{\varkappa\varkappa'} = C_{\rm Ising}\lambda$, with $C_{\rm Ising} \sim 1$ being determined by the geometry. This condition defines a line in the plane of the control parameters, the driving amplitude F and frequency ω_F of the field, since both $J_{\varkappa\varkappa'}$ and λ depend on F and ω_F. The position of this line depends on the strength of the coupling between the oscillators, with $J_{\varkappa\varkappa'} \propto \varepsilon_{\varkappa\varkappa'}$, and also on the oscillator decay rate. The symmetry is broken on one side of the line, whereas on the other side the system is "paramagnetic", i.e., the phases of the oscillators are not correlated.

In the case where $\varepsilon_{\varkappa\varkappa'}$ are negative, Eq. (18) maps the system of parametric oscillators onto an antiferromagnetic Ising system. We emphasize that in the system of oscillators that are currently studied, both the strength of the coupling, and often its sign, can be independently controlled.

Importantly, if the oscillators are slightly different, implying $J_{\varkappa\varkappa'} \neq J_{\varkappa'\varkappa}$, the system lacks detailed balance, generally. Indeed, consider the probability of a pair of switching events that bring the system from the state with given $(\sigma_\varkappa, \sigma_{\varkappa'})$ to $(-\sigma_\varkappa, -\sigma_{\varkappa'})$. It is easy to see that this probability depends on which of the spins, $\varkappa$ or $\varkappa'$, switches first for $J_{\varkappa\varkappa'} \neq J_{\varkappa'\varkappa}$. The violation of detailed balance is a generic feature of systems far from thermal equilibrium, and the system of different driven oscillators is in this category. We expect that the time symmetry breaking transition can still occur if the disorder is weak, but the full analysis of this transition is beyond the scope of this paper.

IV. VICINITY OF THE BIFURCATION POINT

To find the coupling parameters $J_{\varkappa\varkappa'}$ one has first to calculate the logarithmic susceptibility of an *isolated oscillator*. A general approach to such a calculation is based on solving the variational problem for the exponent of the switching rate $R_{\sigma_\varkappa}$, which can be formulated using the master equation, Eq. (10). We will consider the limiting cases where simpler approaches can be used. One of them is where the dissipation-induced broadening of the quasienergy levels is much smaller than the level spacing. The corresponding theory is somewhat involved and is described in Appendix A. It reduces the problem to algebraic equations and Fourier transformations that generally require a numerical evaluation.

A. The low-damping limit

Explicit expressions for $J_{\varkappa\varkappa'}$ can be obtained in the vicinity of the bifurcation point μ_B. Here, two regions have to be analyzed separately. One is the case where the spacing of the eigenvalues of $g_\varkappa$ is small compared to λ, even though it still largely exceeds the scaled broadening $\lambda\kappa$ of the quasienergy levels (the quasienergy level broadening is $\sim \hbar\Gamma$, in dimensional units). The other is where the level broadening becomes significantly larger than the level spacing. The first case is outlined in Appendix A. Using the results obtained there, in particular Eq. (A6), we find

$$\chi_{Q\varkappa} = 2(\mu_\varkappa + 1)^{1/2}/(2\bar{n} + 1) \,, \qquad \mu_\varkappa + 1 \ll 1 \,, \qquad J_{\varkappa\varkappa'} = [2/(2\bar{n} + 1)] V_{\varkappa\varkappa'} Q_\varkappa^{(0)} Q_{\varkappa'}^{(0)} \,. \tag{19}$$

The expression (19) for the "spin-coupling" parameters $J_{\varkappa\varkappa'}$ is bilinear in the positions of the wells of the coupled oscillators $Q_\varkappa^{(0)} \approx (\mu_\varkappa - \mu_B)^{1/2} \approx (\mu_\varkappa + 1)^{1/2}$, see Eq. (13) for $\kappa \ll 1$. It is symmetric even in the presence of a weak disorder in the oscillator eigenfrequencies, $J_{\varkappa\varkappa'} = J_{\varkappa'\varkappa}$. Therefore the system of coupled parametric oscillators maps onto the equilibrium Ising model.

B. Classical limit

The condition of applicability of Eq. (A6) holds also far from the bifurcation point if the temperature is high,

$\bar{n} \gg 1$. The logarithmic susceptibility as a function of the only parameter $\mu_\varkappa$ in this case was found in Ref.[41]. It is important that it is not proportional to $Q_\varkappa^{(0)}$. Therefore in the classical limit $J_{\varkappa\varkappa'} \neq J_{\varkappa'\varkappa}$ and the system of coupled parametric oscillators does *not* map on the Ising model if the oscillators are different.

C. The soft-mode controlled dynamics

The role of dissipation becomes increasingly more important as the parameters of an isolated damped oscillator approach the bifurcation point $\mu_B = -(1-\kappa^2)^{1/2}$, see Eq. (13). For $\mu_\varkappa - \mu_B \ll \kappa$, the logarithmic susceptibility in the classical limit was calculated in Ref.[41]. The quantum dynamics near the bifurcation point is similar to the classical dynamics[38]. It is fully controlled by a soft mode, see below. Therefore one can show that the expression for the quantum logarithmic susceptibility is similar to that for the classical one, which allows finding the parameters $J_{\varkappa\varkappa'}$ for weakly coupled oscillators.

A better insight can be gained by formulating the problem of coupled oscillators somewhat differently. We will assume that all oscillators are close to the bifurcation point, i.e., that the condition $\mu_\varkappa - \mu_B \ll \kappa$ holds for all $\varkappa$. It is then convenient to rotate the variables by changing to the new coordinates and momenta $\tilde{Q}_\varkappa$, $\tilde{P}_\varkappa$. They are defined by $\tilde{Q}_\varkappa + i\tilde{P}_\varkappa = (Q_\varkappa + iP_\varkappa)\exp(-i\beta)$ with $\beta = (\pi - \arcsin\kappa)/2$. In these variables,

$$g_\varkappa = \frac{1}{4}(\tilde{Q}_\varkappa^2 + \tilde{P}_\varkappa^2 - \mu)^2 + \frac{1}{2}(\tilde{P}_\varkappa^2 - \tilde{Q}_\varkappa^2)\cos 2\beta + \tilde{P}_\varkappa\tilde{Q}_\varkappa \sin 2\beta - \mu^2/4\,, \tag{20}$$

and $g_c = -\frac{1}{2}\sum_{\varkappa\neq\varkappa'} V_{\varkappa\varkappa'}(\tilde{Q}_\varkappa\tilde{Q}_{\varkappa'} + \tilde{P}_\varkappa\tilde{P}_{\varkappa'})$.

Rewriting Eq. (11) in the new variables, one immediately finds that, over a dimensionless time $(2\kappa)^{-1}$, the variable $\tilde{P}_\varkappa$ relaxes to its quasiequilibrium value $\tilde{P}_\varkappa \approx (\mu_B/\kappa)\tilde{Q}_\varkappa - \sum_{\varkappa'}{}' V_{\varkappa\varkappa'}\tilde{Q}_{\varkappa'}/2\kappa$, whereas the relaxation of $\tilde{Q}_\varkappa$ is much slower. Such a separation of time scales is characteristic of the dynamics near a bifurcation point of a single dynamical system[43]. The variable $\tilde{Q}_\varkappa$ is the analog of a soft mode. Its fluctuations are much stronger than the fluctuations of $\tilde{P}_\varkappa$. In other words, if one writes down the master equation in the Wigner representation, the distribution over $\tilde{P}_\varkappa$ is much narrower than over $\tilde{Q}_\varkappa$, see[38]. One can disregard the fluctuations of $\tilde{P}_\varkappa$, and then the problem is reduced to the dynamics of one variable per oscillator. To leading order in $\mu_\varkappa - \mu_B$ the Langevin equations (11) take the particularly simple and intuitive form

$$\frac{d}{d\tau}\tilde{Q}_\varkappa \approx -\frac{\partial\mathbb{U}(\{\tilde{Q}_\varkappa\})}{\partial\tilde{Q}_\varkappa} + \tilde{f}_\varkappa(\tau)\,,$$
$$\mathbb{U}(\{\tilde{Q}_\varkappa\}) = \frac{|\mu_B|}{\kappa}\sum_\varkappa\left[-\frac{1}{2}(\mu_\varkappa - \mu_B)\tilde{Q}_\varkappa^2 + \frac{1}{4\kappa^2}\tilde{Q}_\varkappa^4\right] - \frac{|\mu_B|}{2\kappa}\sum_{\varkappa\neq\varkappa'} V_{\varkappa\varkappa'}\tilde{Q}_\varkappa\tilde{Q}_{\varkappa'}\,, \tag{21}$$

where $\tilde{f}_\varkappa = f_{Q_\varkappa}\cos\beta + f_{P_\varkappa}\sin\beta$ is a δ-correlated noise with $\langle\tilde{f}_\varkappa(\tau)\tilde{f}_{\varkappa'}(\tau')\rangle = 2D\delta(\tau-\tau')\delta_{\varkappa\varkappa'}$, cf. Eq. (12). Importantly, $\tilde{f}_\varkappa$ can be considered to be a c-number, because there is only one component of the noise for each oscillator. Moreover, since the dynamics of each oscillator is described by only one variable, this dynamics is *classical*. The only trace of the quantum formulation is that the noise intensity D is proportional to $\hbar$ for small $\bar{n}$, cf. Eq. (12).

Equation (21) shows that, near the bifurcation point, the dynamics of coupled quantum parametric oscillators in the rotating frame maps onto the dynamics of a system of coupled overdamped Brownian particles. Each particle moves in a quartic bistable potential, and the coupling between the particles is bilinear in their coordinates.

1. The weak-coupling limit

The behavior of the system (21) strongly depends on the relation between two small parameters: the coupling strength $|V_{\varkappa\varkappa'}|$ and the distance to the bifurcation point $\mu_\varkappa - \mu_B$. The results are particularly simple if $|V_{\varkappa\varkappa'}| \ll \mu_\varkappa - \mu_B$ for all $\varkappa$. Here, in the absence of coupling to other oscillators, the stable states of a $\varkappa$th oscillator are $\sigma_\varkappa\tilde{Q}_\varkappa^{(0)}$,

$$\tilde{Q}_\varkappa^{(0)} = \kappa(\mu_\varkappa - \mu_B)^{1/2}\,. \tag{22}$$

The noise $\tilde{f}_\varkappa$ leads to switching between the states $\sigma_\varkappa = \pm 1$. The coupling to other oscillators modifies the switching rate $W_{\sigma_\varkappa}$. As discussed earlier, for weak noise intensity switching events are rare and, most likely, when one oscillator switches, the oscillators it is coupled to are close to their equilibrium positions (22). Then, the switching rate is given by the Kramers expression[40] for a thermally activated transition over a potential barrier, except that in the case considered here the origin of the fluctuations is quantum[38]. To lowest order in $V_{\varkappa\varkappa'}$,

$$W_{\sigma_\varkappa} = C_\varkappa\exp[-R_{\sigma_\varkappa}/\lambda]\,, \qquad R_{\sigma_\varkappa} = R_\varkappa^{(0)} + \Delta R_{\sigma_\varkappa}\,,$$
$$R_\varkappa^{(0)} = \frac{|\mu_B|(\mu_\varkappa - \mu_B)^2}{2(2\bar{n}+1)}\,, \quad \Delta R_{\sigma_\varkappa} = \sigma_\varkappa\sum_{\varkappa'}{}' J_{\varkappa\varkappa'}\sigma_{\varkappa'}\,,$$
$$J_{\varkappa\varkappa'} = 2V_{\varkappa\varkappa'}|\mu_B\tilde{Q}_\varkappa^{(0)}\tilde{Q}_{\varkappa'}^{(0)}|/\kappa^2(2\bar{n}+1)\,. \tag{23}$$

The prefactor in the switching rate in dimensionless time is $C_\varkappa = |\mu_B|(\mu_\varkappa - \mu_B)/(\sqrt{2}\,\pi\kappa)$. We note that, somewhat

unexpectedly, Eq. (23) for $J_{\varkappa\varkappa'}$, obtained for $\kappa \gg \mu_\varkappa - \mu_B$, goes over into Eq. (19) for $J_{\varkappa\varkappa'}$ obtained for $\kappa \to 0$.

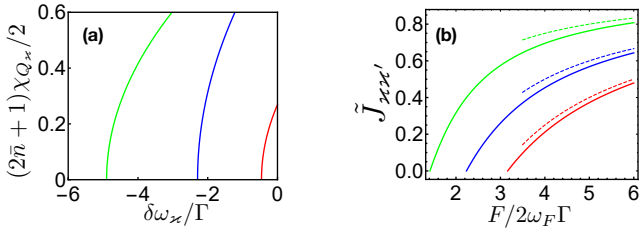

FIG. 3. (a) Logarithmic susceptibility near the bifurcation point as a function of the frequency detuning $\delta\omega_\varkappa/\Gamma \equiv \mu_\varkappa/\kappa$ scaled by the decay rate of the amplitude of free vibrations in unscaled time Γ. For the red, blue, and green curves the scaled field amplitude is $F/2\omega_F\Gamma \equiv \kappa^{-1} = 1.1, 2.5$ and 5. (b) Scaled coupling parameter $\tilde{J}_{\varkappa\varkappa'} = (2\bar{n}+1)J_{\varkappa\varkappa'}/2V_{\varkappa\varkappa'}$ as a function of the field amplitude, Eq.(23). For the red, blue, and green curves the frequency detuning is $\delta\omega_\varkappa/\Gamma = \delta\omega_{\varkappa'}/\Gamma = -3, -2$, and -1. The dashed lines show are given by Eq. (19), which refers to the weak-damping limit.

Equation (23) can be obtained also using the logarithmic susceptibility near the bifurcation point. The dependence of the logarithmic susceptibility on the frequency detuning $\delta\omega_\varkappa = \frac{1}{2}\omega_F - \omega_\varkappa$ for different field amplitude is shown in Fig. 3 (a). Figure 3(b) shows the dependence of the parameters of the effective spin coupling on the field amplitude for different detuning.

We note that, in the soft-mode controlled region, even where the oscillators are somewhat different, still $J_{\varkappa\varkappa'} = J_{\varkappa'\varkappa}$. Therefore the stationary distribution of the system of coupled parametric oscillators coincides with that of the Ising model. Importantly, the correction $\Delta R_{\sigma_\varkappa}$ falls off slower than $R_\varkappa^{(0)}$ as the oscillator approaches the bifurcation point and $\mu_\varkappa - \mu_B$ decreases. This means that the role of the coupling increases closer to the bifurcation point.

D. Stronger coupling: a "time glass"

Sufficiently close to the bifurcation point the weak-coupling condition $|V_{\varkappa\varkappa'}| \ll \mu_\varkappa - \mu_B$ breaks down for many, if not for all oscillators $\varkappa$. If this happens, i.e., if the coupling is stronger, but still $|V_{\varkappa\varkappa'}| \ll |\mu_B|$ [as seen from Eq. (13), $|\mu_B| < 1$], the dynamics of the coupled oscillators near the bifurcation point is described by Eq. (21), except that now this equation cannot be solved by perturbation theory in $V_{\varkappa\varkappa'}$.

In the absence of noise, Eq. (21) has stable stationary solutions, which are inversion-symmetric ($\tilde{Q}_\varkappa \to -\tilde{Q}_\varkappa$), as expected, and correspond to the broken time-translation symmetry. However, these are no longer weakly perturbed single-oscillator states (22). Rather, these states are formed as a result of the coupling. They are located at the minima of the potential "landscape" $\mathbb{U}(\{\tilde{Q}_\varkappa\})$. Generally, if the oscillators are different, this landscape has multiple minima with depth $\sim \kappa|\mu_B|V_{\varkappa\varkappa'}^2$, as seen from Eq. (21). If this depth largely exceeds the noise intensity $D = \lambda\kappa(2\bar{n}+1)/2$, once the system is near a minimum, it will stay there for a long time. This would mean that we can have various types of *many-body* metastable broken-symmetry states, a spin-glass analog in the time domain.

V. QUANTUM PHASE TRANSITION IN THE LATTICE OF PARAMETRIC OSCILLATORS

A. Many-body "ground" state

We now consider a closed system of quantum parametric oscillators, i.e., we assume that the oscillators are isolated from a thermal reservoir. For a single quantum oscillator, the possibility to have a broken-symmetry state is a consequence of the exact degeneracy of the eigenvalues of $g_\varkappa$ for a discrete set of the values of the ratio $\mu_\varkappa/\lambda$[36]. A combination of the corresponding eigenstates is a period-2 state.

For a system of coupled oscillators the situation is different. We will consider the simplest case where the oscillators are identical, form a periodic lattice, and the coupling is ferromagnetic. To allow for two- or three-dimensional systems, we will index the oscillators by a vector $\boldsymbol{\varkappa}$, which can be thought of as the position of the corresponding oscillator. Our primary interest will be the spectrum of excitations in the system and how it evolves on varying the control parameter μ, which is now the same for all oscillators, $\mu_{\boldsymbol{\varkappa}} = \mu$.

The extrema of the RWA Hamiltonian (6) $\mathbb{G}(Q_{\boldsymbol{\varkappa}}, P_{\boldsymbol{\varkappa}}\})$ of the coupled oscillators are given by the equation

$$Q_{\boldsymbol{\varkappa}}(Q_{\boldsymbol{\varkappa}}^2 + P_{\boldsymbol{\varkappa}}^2 - \mu - 1) - \sum_{\boldsymbol{\varkappa}'}{}' V_{\boldsymbol{\varkappa}\boldsymbol{\varkappa}'} Q_{\boldsymbol{\varkappa}'} = 0\,,$$
$$P_{\boldsymbol{\varkappa}}(Q_{\boldsymbol{\varkappa}}^2 + P_{\boldsymbol{\varkappa}}^2 - \mu + 1) - \sum_{\boldsymbol{\varkappa}'}{}' V_{\boldsymbol{\varkappa}\boldsymbol{\varkappa}'} P_{\boldsymbol{\varkappa}'} = 0\,. \qquad (24)$$

For a strongly detuned or weak driving field, $-\mu \gg 1$, the oscillators are prepared in their quantum ground state. Because of the quantum smearing, this makes the system qualitatively different from the corresponding classical system. However, the solution of the above equation for the equilibrium position of the oscillators has the same form as in the classical limit,

$$Q_{\boldsymbol{\varkappa}}^{(0)} = P_{\boldsymbol{\varkappa}}^{(0)} = 0, \qquad \mathbb{G}^{(0)} = 0 \quad (\mu < \mu_{\rm QPT})\,, \qquad (25)$$

where $\mu_{\rm QPT}$ is defined below in Eq. (28); we disregard quantum corrections to $\mathbb{G}^{(0)}$. Excitations in this regime can be obtained by linearizing the equations of motion $\dot{Q}_{\boldsymbol{\varkappa}} = \partial\mathbb{G}/\partial P_{\boldsymbol{\varkappa}}$, $\dot{P}_{\boldsymbol{\varkappa}} = -\partial\mathbb{G}/\partial Q_{\boldsymbol{\varkappa}}$ about $Q_{\boldsymbol{\varkappa}}^{(0)} = P_{\boldsymbol{\varkappa}}^{(0)} = 0$ and seeking the solution for the increments of $Q_{\boldsymbol{\varkappa}}$, $P_{\boldsymbol{\varkappa}}$ in the standard form $\delta Q_{\boldsymbol{\varkappa}} = \delta Q(\mathbf{k})\exp(i\mathbf{k}\boldsymbol{\varkappa})$, $\delta P_{\boldsymbol{\varkappa}} = \delta P(\mathbf{k})\exp(i\mathbf{k}\boldsymbol{\varkappa})$. The excitations are "optical phonons"

with frequencies

$$\omega^{(0)}(\mathbf{k}) = \left\{[\mu + V(\mathbf{k})]^2 - 1\right\}^{1/2} ,$$
$$V(\mathbf{k}) = \sum_{\boldsymbol{\varkappa}'}{}' V_{\boldsymbol{\varkappa}\boldsymbol{\varkappa}'} \exp[i\mathbf{k}(\boldsymbol{\varkappa}' - \boldsymbol{\varkappa})] . \qquad (26)$$

The Fourier components of the coupling parameters have the property $V(\mathbf{k}) = V^*(\mathbf{k})$: this is because $V_{\boldsymbol{\varkappa}\boldsymbol{\varkappa}'} = V_{\boldsymbol{\varkappa}'\boldsymbol{\varkappa}}$ and $V_{\boldsymbol{\varkappa}\boldsymbol{\varkappa}'}$ is translationally invariant. Thus, for sufficiently large $-\mu$, the frequencies (26) are real. They correspond to the (scaled) frequencies of the undriven coupled oscillators with the Hamiltonian $H_0 + H_c$, Eqs. (2) and (4), shifted by $-\omega_F/2$. We note that there is only one branch of phonons in the system of coupled oscillators even in the absence of the periodic drive, as each oscillator has only one degree of freedom.

The spectrum (26) is gapped, as illustrated in the left panel in Fig. 2. For small k,

$$\omega^{(0)}(\mathbf{k}) \approx \omega^{(0)}(0) - \frac{\mu + V(0)}{2\omega^{(0)}} \sum_{\boldsymbol{\varkappa}'}{}' V_{\boldsymbol{\varkappa}\boldsymbol{\varkappa}'} [\mathbf{k}(\boldsymbol{\varkappa} - \boldsymbol{\varkappa}')]^2 ,$$
$$\omega^{(0)}(0) = [(2 + \mu_{\rm QPT} - \mu)(\mu_{\rm QPT} - \mu)]^{1/2} \quad (\mu < \mu_{\rm QPT}) , \qquad (27)$$

where

$$\mu_{\rm QPT} = -1 - V(\mathbf{0}) \qquad (28)$$

(we note that $\mu_{\rm QPT} < -1$).

As μ increases and approaches $\mu_{\rm QPT}$, the spectral gap $\omega^{(0)}(0)$ decreases. For $\mu = \mu_{\rm QPT}$ the gap goes to zero and the spectrum of the Floquet phonons becomes linear for $k \to 0$, see the central panel in Fig. 2: $\omega^{(0)}(\mathbf{k}) \to \omega_{\rm QPT}(\mathbf{k})$. For small k

$$\omega_{\rm QPT}(\mathbf{k}) \approx \left\{ \sum_{\boldsymbol{\varkappa}'}{}' V_{\boldsymbol{\varkappa}\boldsymbol{\varkappa}'} [\mathbf{k}(\boldsymbol{\varkappa} - \boldsymbol{\varkappa}')]^2 \right\}^{1/2} \propto k . \qquad (29)$$

For $\mu > \mu_{\rm QPT}$ the extremum (25) is no longer the minimum of the RWA Hamiltonian $\mathbb{G}$. As seen from Eq. (24), $\mathbb{G}$ has two equally deep minima of depth $\mathbb{G}^{(0)}$, which are located at

$$Q_{\boldsymbol{\varkappa}} = \pm Q^{(0)} , \; P_{\boldsymbol{\varkappa}} = 0 ; \qquad Q^{(0)} = (\mu - \mu_{\rm QPT})^{1/2} ,$$
$$\mathbb{G}^{(0)} = -(\mu - \mu_{\rm QPT})^2/4 \quad (\mu > \mu_{\rm QPT}) . \qquad (30)$$

We checked numerically for short chains with nearest-neighbor coupling that Eq. (30) provides the global minimum of $\mathbb{G}$.

The solution (30) describes two degenerate quantum-coherent period-2 states of the system of coupled oscillators. Excitations about these states can be found by linearizing the quantum equations of motion for $Q_{\boldsymbol{\varkappa}}$ and $P_{\boldsymbol{\varkappa}}$, as it was done above for excitations about the state (25). The frequencies of the corresponding Floquet phonons are

$$\omega^{(0)}(\mathbf{k}) = [1 - \mu_{\rm QPT} - V(\mathbf{k})]^{1/2}$$
$$\times [2(\mu - \mu_{\rm QPT}) + V(\mathbf{0}) - V(\mathbf{k})]^{1/2} \quad (\mu > \mu_{\rm QPT}) . \qquad (31)$$

The spectrum (31) is gapped, cf. the right panel in Fig. 2, with $\omega^{(0)}(\mathbf{0}) = 2(\mu - \mu_{\rm QPT})^{1/2}$; the difference $\omega^{(0)}(\mathbf{k}) - \omega^{(0)}(\mathbf{0})$ is quadratic in k for small k, as in the case $\mu < \mu_{\rm QPT}$.

The evolution of the system as μ increases from below to above $\mu_{\rm QPT}$ corresponds to a quantum phase transition to a many-body period-2 state. In the rotating frame, one can think of it in terms of the wave function as a function of the coordinates $\{Q_{\boldsymbol{\varkappa}}\}$. In the symmetric phase this wave function is almost even with respect to each coordinate $Q_{\boldsymbol{\varkappa}}$ and is maximal for all $Q_{\boldsymbol{\varkappa}} = 0$. The admixture of terms that are not even with respect to individual $Q_{\boldsymbol{\varkappa}}$ is small. This is reminiscent of the paramagnetic state of an Ising spin chain in a strong transverse field, where each spin is almost completely aligned along the field. On the other hand, in the symmetry broken phase, the wave function of our system is close to the product of the wave functions of the individual oscillators centered either at $Q^{(0)}$ or at $-Q^{(0)}$. The tunnel splitting between the states that are symmetric and antisymmetric combinations of such products is exponentially small in the size of the system. This again reminds a spin chain with the eigenstates $|\uparrow\uparrow\ldots\rangle$ and $|\downarrow\downarrow\ldots\rangle$.

The transition is determined by quantum fluctuations. If the evolution occurs as μ is slowly increased in time, it should have the familiar features associated with the creation of topological defects due to the nonadiabaticity that occurs where the excitation gap approaches zero, see[44,45]. In this region quantum effects related to the nonlinearity of the oscillators become important, too. We emphasize again that the broken-symmetry state in $\{Q_{\boldsymbol{\varkappa}}\}$-space corresponds to the state with a broken time-translation symmetry in the lab frame.

The critical point can be traversed by changing the frequency or the amplitude of the driving force (or both). The parameter scaling used above was done assuming a nonzero field amplitude. An alternative scaling that allows turning the field on from zero is described in Appendix B.

VI. CONCLUSIONS

The results of this paper show that the Floquet dynamics of coupled quantum oscillators can exhibit a breaking of the discrete time-translation symmetry imposed by a periodic field. This symmetry breaking occurs when the frequency of the driving field is close to twice the eigenfrequencies of the oscillators. In the broken-symmetry state the phases of the parametrically excited vibrations of different oscillators take correlated values; the system has an equivalent state where all these phases differ by π. This can be contrasted with the case of uncoupled oscillators: here, the vibration phases are uncorrelated and on average the symmetry in a large system is not broken.

Because the energy spectrum of the system of coupled oscillators consists of narrow slightly nonequidistant bands, the resonant driving required for the symmetry

breaking is weak. The drive frequency largely exceeds the width of the bands, preventing uncontrolled intraband heating. Moreover, the driving does not induce decay processes with participation of excitations of the bath known in quantum optomechanics as sideband heating[46]. Therefore disorder is not necessary for avoiding heating and observing coherent many-body effects. It is well-known experimentally that heating is not an issue for a single parametrically excited cavity mode or a nanoresonator, and there is no reason to expect that it would become an issue for coupled oscillators.

Transitions between the degenerate broken-symmetry states of the periodically-driven system correspond to phase slips. For a many-body state, collective phase slips are rare and the lifetime of the broken-symmetry state scales exponentially with the size of the system even for weak coupling between the oscillators.

In contrast to a single quantum-coherent (non-dissipative) parametric oscillator, where symmetry breaking is possible but requires fine tuning of the interrelation between the amplitude and frequency of the driving field[35], for coherent coupled oscillators no fine-tuning is needed. The symmetry-breaking transition in this case is a quantum phase transition. It occurs as the amplitude or frequency of the driving field go across the corresponding critical values (which differ from the bifurcational parameter values of an isolated oscillator).

In the presence of dissipation, an individual oscillator $\varkappa$ has two metastable broken-symmetry states with opposite phases. Quantum fluctuations lead to transitions between these states. The oscillator-oscillator coupling modifies the rates of these transitions. Remarkably, for a weak coupling, the rates can be found using the logarithmic susceptibility of an isolated oscillator that describes its response to a weak extra field.

In Fig. 4 we sketch the different regimes where we have obtained explicit results – they are also summarized below in this section. The parameter κ in the figure is related to the friction coefficient Γ of an oscillator as $\kappa = 2\Gamma\omega_F/F$; here F and ω_F are the amplitude and frequency of the parametric drive, and Γ is the decay rate of the (free) vibration amplitude. From the linearized equations of motion Eq. (11) one can see that the boundary between the regimes where the motion of an isolated oscillator in the rotating frame changes character is given by the condition

$$\mu - \mu_B = -\kappa^2/2\mu_B.$$

Well below this boundary on the (κ^{-1}, μ)-plane (but for $\mu > \mu_B$) the motion near the stable states of an oscillator is controlled by a soft mode. On the other hand, for $\mu - \mu_B \gg -\kappa^2/2\mu_B$ the spacing of the quasienergy levels largely exceeds their width. The results in this range apply also for $-\mu_B > \mu > 0$.

The concept of the logarithmic susceptibility allows one to map coupled oscillators on a system of coupled spins $\{\sigma_\varkappa\}$. The different broken-symmetry states of an oscillator $\varkappa$ correspond to different values $\sigma_\varkappa = \pm 1$. If

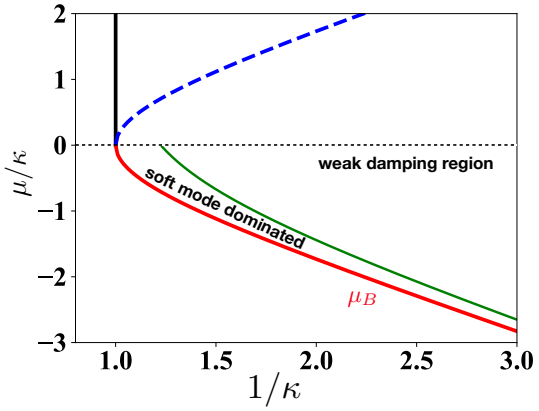

FIG. 4. The characteristic parameter regions of a parametric oscillator on the plane $(\kappa^{-1}, \mu/\kappa)$. The variable κ^{-1} is proportional to the driving amplitude F, whereas $\mu/\kappa \propto \delta\omega/\Gamma$ depends on ω_F, but not on F. The period-two states emerge on the bold red line $\mu_B = -(1-\kappa^2)^{1/2}$ and also on the vertical black line. The dashed blue line shows the bifurcation line $-\mu_B$ where the zero-amplitude state becomes stable. The green line, $\mu = \mu_B - \kappa^2/2\mu_B$ bounds the region near the bifurcation line where the motion near the stable states in the rotating frame is overdamped. Well inside this region the results are described by Eqs. (21) – (23). Well above the green line the spacing of the quasienergy levels exceeds their width and the results are described by the theory of Appendix A and Eq. (19). Further in the region of large κ^{-1} the dissipation can be disregarded and the quantum phase transition physics comes into play.

the system is large and the coupling is not too weak, a stationary state is formed where the phases of all oscillators (the values of $\sigma_\varkappa$ with different $\varkappa$) are correlated. Overall, in the absence of disorder the system is mapped onto the Ising model with the coupling not necessarily limited to the nearest neighbors. A broken-symmetry state emerges if the effective dimension of the system, which is determined by the connectivity, is larger than one. The effective temperature of the system is $\propto \hbar$ if the oscillator Planck number $\bar{n} \lesssim 1$ and goes over into T for $\bar{n} \gg 1$. The mapping applies if the spin coupling parameters $J_{\varkappa\varkappa'}$ exceed the effective temperature.

The parameters $J_{\varkappa\varkappa'}$ have a different form depending on the distance from the bifurcation point. They have been found in explicit form close to the bifurcation line in Fig. 4 sufficiently well below and well above the green line, see Sec. IV. The corresponding expressions match in the crossover region. Further away from the bifurcation line, finding $J_{\varkappa\varkappa'}$ requires numerical calculations that are outlined in Appendix A.

The mapping on coupled spins applies not only if the oscillators are identical, but also if they are slightly different, i.e., if the system is disordered. Two kinds of disorder can be distinguished. One is a disorder in the coupling matrix elements $\varepsilon_{\varkappa\varkappa'} \propto V_{\varkappa\varkappa'}$ of the oscillators. In this case the stationary distribution is still given by that of the Ising model with the corresponding

$J_{\varkappa\varkappa'} = J_{\varkappa'\varkappa} \propto V_{\varkappa\varkappa'}$. The other case is where the oscillators themselves are different, for example, have slightly different eigenfrequencies. Interestingly, close to the bifurcation line in Fig. 4 the stationary distribution in this case is described by that of the Ising model as well.

Further away from the bifurcation line the mapping onto the Ising model breaks down for differing oscillators, even though one can still map the oscillators onto coupled spins. Here the spin dynamics lacks detailed balance. In the stationary state, there is a microscopic current in "spin space". This is a consequence of the oscillators being far from thermal equilibrium. To the best of our knowledge, the dynamics of Ising spins in the absence of detailed balance has not been explored. Coupled parametric oscillators provide a platform for studying this dynamics.

Another qualitatively different regime occurs if the oscillators are close to the bifurcation line but their coupling may no longer be assumed weak. Such a regime invariably emerges as the bifurcation line is approached: There, each oscillator becomes more and more sensitive to perturbations, including coupling to other oscillators. In this regime the dynamics can be mapped onto that of coupled overdamped Brownian particles driven by noise with the intensity $\propto \hbar$, for low temperatures. In the presence of disorder, the resulting "potential landscape" has multiple metastable minima. Each of them corresponds to a broken time symmetry state of the system.

The rich pattern of symmetry-broken states described here and the possibility of controlling them by varying the parameters of the driving field makes the system of parametric quantum oscillators attractive for studying quantum "time-crystal" phenomena. As mentioned in the introduction, an appropriate platform for such studies is provided, for example, by various well-characterized mesoscopic oscillatory systems with controlled coupling between the modes. Our results bear not only on the issue of time symmetry breaking, but also on general questions of quantum physics far from thermal equilibrium, including such important problems as nonequilibrium quantum phase transitions, quantum-fluctuation induced microscopic currents in the stationary state, and quantum diffusion in a potential landscape.

ACKNOWLEDGMENTS

MID acknowledges the warm hospitality at the University of Konstanz and the partial support from the DFG through SFB 767 *Controlled Nanosystems* and from the Zukunftskolleg Senior Fellowship. His research was also supported by the National Science Foundation (Grant No. DMR-1806473). CB and NL acknowledge financial support by the Swiss SNF and the NCCR Quantum Science and Technology. Y.Z. was supported by the National Science Foundation (DMR-1609326).

Appendix A: Quantum logarithmic susceptibility

In the weak-damping limit, we write the master equation (10) for the isolated oscillator $\varkappa$ as a balance equation for the populations $\rho_{m_\varkappa}$ of the eigenstates $|m_\varkappa\rangle$ of the RWA Hamiltonian

$$G_\varkappa = g_\varkappa + \Delta g_\varkappa \,. \tag{A1}$$

The operator $G_\varkappa$ describes an isolated parametric oscillator $\varkappa$ driven additionally by a weak field at half the frequency of the parametric drive. The term $\Delta g_\varkappa$ is given by Eq. (14); it is proportional to the weak field amplitude F'.

For small λ and F', the function $G_\varkappa(Q_\varkappa, P_\varkappa)$ has two slightly asymmetric wells (enumerated by $\sigma_\varkappa = \pm 1$), cf. Fig. 1(d). There are many eigenstates inside each of the wells for $\lambda \ll 1$. We consider the states $|m_\varkappa\rangle$ inside one of the wells and number them so that $m_\varkappa = 0$ corresponds to the lowest state. Coupling to a thermal reservoir leads to transitions $|m_\varkappa + k_\varkappa\rangle \to |m_\varkappa\rangle$. From Eq. (10), the rates $\Lambda_{m_\varkappa+k_\varkappa\, m_\varkappa}$ of such intrawell transitions are given by the squared matrix elements of the operators $a_\varkappa, a_\varkappa^\dagger$ on the corresponding wave functions,

$$\begin{aligned}\Lambda_{m_\varkappa+k_\varkappa\, m_\varkappa} &= 2\kappa(\bar n+1)\,|\langle m_\varkappa|a_\varkappa|m_\varkappa+k_\varkappa\rangle|^2 \\ &\quad + 2\kappa\bar n\,|\langle m_\varkappa+k_\varkappa|a_\varkappa|m_\varkappa\rangle|^2 \,. \end{aligned}\tag{A2}$$

Generally, the rates of transitions with $k_\varkappa > 0$ are higher than with $k_\varkappa < 0$. Then the system is more likely to move to eigenstates with lower $G_\varkappa$. This corresponds to the minima of $G_\varkappa(Q_\varkappa, P_\varkappa)$ being stable states of the oscillator in the classical limit.

However, even for zero temperature, in contrast to equilibrium systems, transitions away from the minima of $G_\varkappa$, i.e., with $k_\varkappa < 0$, have nonzero rates. They lead to the probability for an oscillator, starting from deep inside of a well, to reach the intrawell states near the top of the barrier of $G_\varkappa$. From there, the oscillator will end up in each of the two wells with probability $\sim 1/2$. The exponent of the switching rate $W_{\sigma_\varkappa}$ is thus determined by the population of the intrawell states $|m_\varkappa\rangle$ of the $\sigma_\varkappa$-well near the top of the barrier. The logarithmic susceptibility describes the linear dependence of the exponent of this population on the field F'.

It is convenient to seek the state populations $\rho_{m_\varkappa}$ in the form $\rho_{m_\varkappa} = \exp[-R\big(G(m_\varkappa)\big)/\lambda]$, where $G(m_\varkappa)$ is the eigenvalue of $G_\varkappa$ in the state $|m_\varkappa\rangle$. This form of $\rho_{m_\varkappa}$ is reminiscent of a Boltzmann distribution, with λ playing the role of the temperature and $R(G)$ playing the role of the energy. In the considered nonequilibrium case, R is not a linear function of G. The populations $\rho_{m_\varkappa}$ strongly vary with the level number $m_\varkappa$. However, generally, the function $R(G)$ is smooth even for small λ.

The equation for $R(G)$ can be obtained from the master equation in the eikonal (WKB) approximation. Equation (A2) shows that the intrawell transition rates $\Lambda_{m_\varkappa+k_\varkappa\, m_\varkappa}$ fall off exponentially fast with $|k_\varkappa|$. One

can then expand $R\big(G(m_\varkappa + k_\varkappa)\big) \approx R\big(G(m_\varkappa)\big) + \lambda k_\varkappa [\omega(G) dR/dG]_{m_\varkappa}$, which is essentially the eikonal approximation. Here, $[\cdot]_{m_\varkappa}$ indicates that the function of G is evaluated for $G = G(m_\varkappa)$; function $\omega(G)$ is the frequency of classical vibrations with a given G. We used that $\omega(G_{m_\varkappa}) = \lambda^{-1}[G(m_\varkappa + 1) - G(m_\varkappa)] + o(\lambda)$.

In deriving the equation for $R(G)$ one should keep in mind that changing $m_\varkappa$ by $k_\varkappa$ in the both subscripts of $\Lambda_{m_\varkappa + k_\varkappa\, m_\varkappa}$ leads to a small change that can be disregarded for $m_\varkappa \gg 1$ and $|k_\varkappa| \ll m_\varkappa$. Yet another fact is that the intrawell distribution $\rho_{m_\varkappa}$ is formed on a timescale $\sim 1/\kappa \ll 1/W_{\sigma_\varkappa}$. Thus, for times $\ll 1/W_{\sigma_\varkappa}$ the populations of the intrawell states are given by the stationary solution of the balance equation. Using these arguments, one can derive from Eq. (10) the balance equation for the intrawell state populations as

$$\sum_{k_\varkappa} \Lambda_{m_\varkappa + k_\varkappa\, m_\varkappa} \left\{ 1 - \exp\left[-k_\varkappa \big[\omega(G) dR/dG\big]_{m_\varkappa} \right] \right\} = 0 \,. \tag{A3}$$

In the WKB approximation that we used, the matrix elements of the lowering operator $a_\varkappa$ in Eq. (A2) can be written as

$$\begin{aligned} a_{k_\varkappa}(m_\varkappa) &\equiv \langle k_\varkappa + m_\varkappa | a_\varkappa | m_\varkappa \rangle \\ &= \frac{1}{2\pi} \int_0^{2\pi} d\phi \exp(-i k_\varkappa \phi) a_\varkappa\big(G(m_\varkappa)\big|\phi\big) \,, \end{aligned} \tag{A4}$$

where $a_\varkappa(G|\phi)$ is the value of $a_\varkappa = (2\lambda)^{-1/2}(Q_\varkappa + iP_\varkappa)$ calculated as a classical function of the phase $\phi = \omega(G)\tau$ on the classical intrawell trajectory with a given G.

Equation (A3) is an algebraic equation for $\pi_\varkappa \equiv \omega(G_\varkappa) dR/dG_\varkappa$. In the absence of an extra drive $\propto F'$, it was derived and solved in Ref.[30]. Importantly, in this equation one can treat $\lambda m_\varkappa \equiv I_\varkappa$ as a continuous variable. To leading order in λ, $\omega(G_\varkappa) = dG_\varkappa/dI_\varkappa$. The variable $I_\varkappa = (2\pi)^{-1} \oint P_\varkappa dQ_\varkappa$ is the classical action for the intrawell orbit with a given $G_\varkappa$. Equation (A3) does not contain the effective Planck constant λ; it gives $\pi_\varkappa = dR/dI_\varkappa$ as a function of the continuous variable $I_\varkappa$.

The change of R due to the perturbation $\Delta g_\varkappa$ can be found by finding the change $\Delta\Lambda_{m_\varkappa + k_\varkappa\, m_\varkappa}$ of the intrawell transition rates compared to their values $\Lambda^{(0)}_{m_\varkappa + k_\varkappa\, m_\varkappa}$ for $\Delta g_\varkappa = 0$. In turn, the rate change comes from the change of the matrix elements $a_{k_\varkappa}(m_\varkappa)$. The correction to $a_{k_\varkappa}(m_\varkappa)$ of first-order in $\Delta g_\varkappa$ can be obtained from Eq. (A4) using the classical equations of motion for $Q_\varkappa, P_\varkappa$ with the perturbed effective Hamiltonian $g_\varkappa(Q_\varkappa, P_\varkappa) + \Delta g_\varkappa(Q_\varkappa, P_\varkappa)$, which is a standard problem of classical nonlinear mechanics[47]. An important simplification is that, in the limit of weak damping, the value of the momentum in a stable state is $P^{(0)}_\varkappa = 0$. Therefore the coupling parameters $J_{\varkappa\varkappa'}$ in Eq. (16) are determined only by the $\chi_{Q_\varkappa}$-component of the logarithmic susceptibility. As a consequence, as seen from Eq. (14), when calculating the correction to $a_{k_\varkappa}(m_\varkappa)$ we can limit the analysis to $\Delta g_\varkappa = -f' Q_\varkappa$, i.e., $\varphi_\varkappa = \pi/2$ in Eqs. (14) and (15).

Since the leading-order corrections to the intrawell transition rates are linear in $f' \propto F'$, so is also the leading-order correction $\Delta\pi_\varkappa(I_\varkappa)$ to the unperturbed value $\pi^{(0)}_\varkappa(I_\varkappa)$. From Eq. (A3) it has the form

$$\begin{aligned} \Delta\pi_\varkappa(I_\varkappa) = &- \sum_{k_\varkappa} \Delta\Lambda_{m_\varkappa + k_\varkappa\, m_\varkappa} \left\{ 1 - \exp[-k_\varkappa \pi^{(0)}_\varkappa(I_\varkappa)] \right\} \\ &\times \left\{ \sum_{k_\varkappa} k_\varkappa \Lambda^{(0)}_{m_\varkappa + k_\varkappa\, m_\varkappa} \exp[-k_\varkappa \pi^{(0)}_\varkappa] \right\}^{-1} , \end{aligned}$$

where $m_\varkappa = I_\varkappa/\lambda$ and the rates $\Lambda^{(0)}$, $\Delta\Lambda$ are considered to be continuous functions of $I_\varkappa$.

The logarithmic susceptibility is

$$\chi_{Q\varkappa} = \frac{1}{f'} \int_0^{I_{\varkappa\,\max}} \Delta\pi_\varkappa(I_\varkappa) dI_\varkappa \,. \tag{A5}$$

As indicated above, it is assumed here that $\Delta\pi_\varkappa$ is calculated for the $\sigma_\varkappa = 1$-well of the oscillator (the well of $g_\varkappa(Q_\varkappa, P_\varkappa)$ with the minimum at $Q^{(0)}_\varkappa > 0$). The upper limit $I_{\varkappa\,\max}$ is the value of the mechanical action in this well at the barrier top of $g_\varkappa$. In the case of weak damping, the logarithmic susceptibility depends on two parameters, $\mu_\varkappa$ and $\bar{n}$. Generally, Eqs. (A5) and (16) suggest that $J_{\varkappa\varkappa'}$ is not symmetric with respect to the interchange $\varkappa \leftrightarrow \varkappa'$ in the presence of disorder in the oscillator system.

In the absence of the drive $\propto F'$, the assumption of R being a smooth function of $g_\varkappa$ breaks down for a certain range of $\mu_\varkappa$ in a very narrow range of temperatures; for a resonantly driven oscillator this range was found to be limited to $\exp(-1/\lambda) \ll \bar{n} \ll \lambda^{3/2}$[48]. It is important that, for $\bar{n} \to 0$, the perturbation $\Delta g_\varkappa$ does not break the smoothness of $R(g_\varkappa)$. One can see this by showing that the exponent of the decay of the intrawell transition rates $\Lambda_{m_\varkappa + k_\varkappa\, m_\varkappa}$ with $|k_\varkappa|$ is weakly modified by a weak perturbation. The analysis of the decay is somewhat involved and will be presented elsewhere. Here we only note that a weak change of the decay exponent of the rates means that the sum over $k_\varkappa$ in Eq. (A3) remains converging rapidly for $R(G_\varkappa)$ close to its value in the absence of the perturbation.

1. Underdamped dynamics near the bifurcation point

The analysis of Eq. (A3) is greatly simplified if $dR/dI_\varkappa \ll 1$. This happens for $\mu_\varkappa$ close to the bifurcation point μ_B, see Eq. (13); in the limit of weak damping, $\mu_B \to -1$. Here one can expand the exponential factor in Eq. (A3) to second order in $dR/dI_\varkappa \equiv \omega(G_\varkappa) dR/dG_\varkappa$. In the absence of an extra drive the calculation was described in[30]. It can be immediately generalized to the case where such a drive is present, as in Eq. (A3). One then finds from Eqs. (A3) and (A4) that, even before the

linearization with respect to f', the resulting expression for $dR/dI_\varkappa$ is similar to that for a classical oscillator,

$$\frac{dR}{dI_\varkappa} = \frac{2\omega(G_\varkappa)}{2\bar{n}+1}\frac{2\pi I_\varkappa}{N(G_\varkappa)}\,, \quad I_\varkappa = \frac{1}{2\pi}\iint dQ_\varkappa dP_\varkappa\,,$$
$$N(G_\varkappa) = \iint dQ_\varkappa dP_\varkappa[2(Q_\varkappa^2+P_\varkappa^2)-\mu_\varkappa]\,. \tag{A6}$$

The integration in the expressions for $N(G_\varkappa)$ and $I_\varkappa$ is done over the interior of the contour $G_\varkappa(Q_\varkappa,P_\varkappa)=G_\varkappa$. Equation (A6) applies near the bifurcation point because the frequency $\omega(G_\varkappa)$ is small, $\omega(G_\varkappa)\le 2\sqrt{\mu_\varkappa+1}\ll 1$ and therefore, as presumed, $dR/dI_\varkappa \ll 1$. We note also that in the expression for $N(G_\varkappa)$, $Q_\varkappa^2$ and $P_\varkappa^2$ are small, which allows one to easily find the ratio $I_\varkappa/N(G_\varkappa)$.

Appendix B: Turning up the driving amplitude

To develop a formulation that will allow us to see how the quantum phase transition occurs on increasing the amplitude of the driving force, we introduce a scaling amplitude F_s. The dimensionless parameters of the dynamics are

$$f_{\rm p} = \frac{F}{F_s}\,, \quad \mu'_\varkappa = \frac{\omega_F(\omega_F-2\omega_\varkappa)}{F_s}{\rm sgn}\gamma\,,$$
$$C' = |2F_s/3\gamma|^{1/2}\,, \quad \lambda' = 3|\gamma|\hbar/\omega_F F_s\,, \tag{B1}$$

and we define the slow variables as $U^\dagger(t)[q_\varkappa + (2i/\omega_F)p_\varkappa]U(t) = -iC'(Q_\varkappa+iP_\varkappa)e^{-i\omega_F t/2}$. This leads to $U^\dagger\,H\,U - i\hbar U^\dagger\dot{U} = (F_s^2/6\gamma)\mathbb{G}'$ with

$$\mathbb{G}' = \sum_\varkappa g'_\varkappa(Q_\varkappa,P_\varkappa) + g'_c\,,$$
$$g'_\varkappa(Q,P) = \frac{1}{4}(P_\varkappa^2+Q_\varkappa^2-\mu'_\varkappa)^2$$
$$+\frac{1}{2}f_{\rm p}(P_\varkappa^2-Q_\varkappa^2) - \frac{1}{4}\mu'^2_\varkappa\,. \tag{B2}$$

Here, g'_c is given by Eq. (8) for g_c in which $V_{\varkappa\varkappa'}$ is replaced with $V'_{\varkappa\varkappa'} = 2\varepsilon_{\varkappa\varkappa'}/F_s$. The dimensionless time τ, in which the RWA dynamics is described by the equation $dA/d\tau = -i(\lambda')^{-1}[A,\mathbb{G}']$, is $\tau = (F_s/2\omega_F)t$.

For ferromagnetic coupling in a periodic system of identical oscillators ($\varkappa\to\boldsymbol{\varkappa}, \mu'_\varkappa\to\mu'$) in the broken-symmetry state we have a minimum of $\mathbb{G}'$ at $Q_{\boldsymbol{\varkappa}} = \pm Q^{(0)\,\prime}$, $P_{\boldsymbol{\varkappa}}=0$, with

$$Q^{(0)\,\prime} = (f_{\rm p}-f_{\rm QPT})^{1/2}, \qquad f_{\rm QPT} = -\mu' - V'(\mathbf{0}),$$
$$\omega(\mathbf{k}) = [2f_{\rm p}+V'(\mathbf{0})-V'(\mathbf{k})]^{1/2}$$
$$\times\,[2f_{\rm p}-2f_{\rm QPT}+V'(\mathbf{0})-V'(\mathbf{k})]^{1/2}. \tag{B3}$$

Here, $V'(\mathbf{k})$ is given by Eq. (31) for $V(\mathbf{k})$ with $V_{\boldsymbol{\varkappa}\boldsymbol{\varkappa}'}$ replaced by $V'_{\boldsymbol{\varkappa}\boldsymbol{\varkappa}'}$.

If μ' is negative and $\mu'+V'(\mathbf{0})<0$, Eq. (B3) leads to a critical value of the scaled driving force amplitude $f_{\rm p}=f_{\rm QPT}=-\mu'-V'(\mathbf{0})$ where $Q^{(0)\,\prime}=0$ and the gap in the excitation spectrum (B3) disappears. The analysis of the case $f_{\rm p}<f_{\rm QPT}$ is fully analogous to that for the case $\mu<\mu_{\rm QPT}$ in Sec. V; in this case $Q^{(0)\,\prime}=0$. The results show explicitly that one can go through the quantum phase transition by either varying the driving frequency or the driving amplitude.

[1] F. Wilczek, Phys. Rev. Lett. **109**, 160401 (2012).
[2] V. Khemani, A. Lazarides, R. Moessner, and S. L. Sondhi, Phys. Rev. Lett. **116**, 250401 (2016).
[3] D. V. Else, B. Bauer, and C. Nayak, Phys. Rev. Lett. **117**, 090402 (2016).
[4] C. W. von Keyserlingk and S. L. Sondhi, Phys. Rev. B **93**, 245146 (2016).
[5] N. Y. Yao, A. C. Potter, I.-D. Potirniche, and A. Vishwanath, Phys. Rev. Lett. **118**, 030401 (2017).
[6] J. Zhang, P. W. Hess, A. Kyprianidis, P. Becker, A. Lee, J. Smith, G. Pagano, I.-D. Potirniche, A. C. Potter, A. Vishwanath, N. Y. Yao, and C. Monroe, Nature **543**, 217 (2017).
[7] S. Choi, J. Choi, R. Landig, G. Kucsko, H. Zhou, J. Isoya, F. Jelezko, S. Onoda, H. Sumiya, V. Khemani, C. von Keyserlingk, N. Y. Yao, E. Demler, and M. D. Lukin, Nature **543**, 221 (2017).
[8] J. Rovny, R. L. Blum, and S. E. Barrett, Phys. Rev. Lett. **120**, 180603 (2018).
[9] W. Berdanier, M. Kolodrubetz, S. A. Parameswaran, and R. Vasseur, Proc. Nat. Acad. Sci. **115**, 9491 (2018).
[10] D. A. Abanin, W. De Roeck, and F. Huveneers, Ann. Phys. **372**, 1 (2016).
[11] P. Bordia, H. Lüschen, U. Schneider, M. Knap, and I. Bloch, Nature Physics **13**, 460 (2017).
[12] D. A. Abanin, W. De Roeck, W. W. Ho, and F. Huveneers, Phys. Rev. B **95** (2017).
[13] K. Kim, M. S. Heo, K. H. Lee, K. Jang, H. R. Noh, D. Kim, and W. Jhe, Phys. Rev. Lett. **96**, 150601 (2006).
[14] M. S. Heo, Y. Kim, K. Kim, G. Moon, J. Lee, H. R. Noh, M. I. Dykman, and W. Jhe, Phys. Rev. E **82**, 031134 (2010).

[15] Z. Wang, A. Marandi, K. Wen, R. L. Byer, and Y. Yamamoto, Phys. Rev. A **88**, 063853 (2013).

[16] P. L. McMahon, A. Marandi, Y. Haribara, R. Hamerly, C. Langrock, S. Tamate, T. Inagaki, H. Takesue, S. Utsunomiya, K. Aihara, R. L. Byer, M. M. Fejer, H. Mabuchi, and Y. Yamamoto, Science **354**, 614 (2016).

[17] T. Inagaki, Y. Haribara, K. Igarashi, T. Sonobe, S. Tamate, T. Honjo, A. Marandi, P. L. McMahon, T. Umeki, K. Enbutsu, O. Tadanaga, H. Takenouchi, K. Aihara, K. Kawarabayashi, K. Inoue, S. Utsunomiya, and H. Takesue, Science **354**, 603 (2016).

[18] I. Mahboob, H. Okamoto, and H. Yamaguchi, Sci. Adv. **2**, e1600236 (2016).

[19] H. Goto, Sci. Rep. **6**, 21686 (2016).

[20] S. E. Nigg, N. Lörch, and R. P. Tiwari, Sci. Adv. **3**, e1602273 (2017).

[21] S. Puri, C. K. Andersen, A. L. Grimsmo, and A. Blais, Nature Communications **8**, 15785 (2017).

[22] H. Goto, Z. Lin, and Y. Nakamura, Sci. Rep. **8**, 7154 (2018).

[23] L. D. Landau and E. M. Lifshitz, *Mechanics*, 3rd ed. (Elsevier, Amsterdam, 2004).

[24] J. W. F. Woo and R. Landauer, IEEE J. Quant. Electr. **QE 7**, 435 (1971).

[25] D. L. Underwood, W. E. Shanks, A. C. Y. Li, L. Ateshian, J. Koch, and A. A. Houck, Phys. Rev. X **6**, 021044 (2016).

[26] A. J. Kollár, M. Fitzpatrick, and A. A. Houck, ArXiv e-prints (2018), arXiv:1802.09549.

[27] M. Kounalakis, C. Dickel, A. Bruno, N. K. Langford, and G. A. Steele, npj Quantum information **4**, 38 (2018).

[28] E. Buks and M. L. Roukes, J. Microelectromech. Syst. **11**, 802 (2002).

[29] W. Fon, M. H. Matheny, J. Li, L. Krayzman, M. C. Cross, R. M. D'Souza, J. P. Crutchfield, and M. L. Roukes, Nano Lett. **17**, 5977 (2017).

[30] M. Marthaler and M. I. Dykman, Phys. Rev. A **73**, 042108 (2006).

[31] E. Lieb, T. Schultz, and D. Mattis, Annals of Physics **16**, 407 (1961).

[32] S. Sachdev, *Quantum Phase Transitions* (Cambridge University Press, Cambridge, 1999).

[33] V. Peano, M. Marthaler, and M. I. Dykman, Phys. Rev. Lett. **109**, 090401 (2012).

[34] L. Guo, M. Marthaler, and G. Schön, Phys. Rev. Lett. **111**, 205303 (2013).

[35] Y. Zhang, J. Gosner, S. M. Girvin, J. Ankerhold, and M. I. Dykman, Phys. Rev. A **96**, 052124 (2017).

[36] M. Marthaler and M. I. Dykman, Phys. Rev. A **76**, 010102R (2007); Y. Zhang and M. I. Dykman, *ibid.* **95**, 053841 (2017).

[37] M. I. Dykman and M. A. Krivoglaz, in *Sov. Phys. Reviews*, Vol. 5, edited by I. M. Khalatnikov (Harwood Academic, New York, 1984) pp. 265–441, web.pa.msu.edu/people/dykman/pub06/DKreview84.pdf.

[38] M. I. Dykman, Phys. Rev. E **75**, 011101 (2007).

[39] H. Watanabe and M. Oshikawa, Phys. Rev. Lett. **114**, 251603 (2015).

[40] H. A. Kramers, Physica (Utrecht) **7**, 284 (1940).

[41] D. Ryvkine and M. I. Dykman, Phys. Rev. E **74**, 061118 (2006).

[42] R. B. Karabalin, R. Lifshitz, M. C. Cross, M. H. Matheny, S. C. Masmanidis, and M. L. Roukes, Phys. Rev. Lett. **106**, 094102 (2011).

[43] J. Guckenheimer and P. Holmes, *Nonlinear Oscillators, Dynamical Systems and Bifurcations of Vector Fields* (Springer-Verlag, New York, 1997).

[44] J. Dziarmaga, Adv. Phys. **59**, 1063 (2010).

[45] A. Polkovnikov, K. Sengupta, A. Silva, and M. Vengalattore, Rev. Mod. Phys. **83**, 863 (2011).

[46] M. Aspelmeyer, T. J. Kippenberg, and F. Marquardt, Rev. Mod. Phys. **86**, 1391 (2014).

[47] V. I. Arnold, *Mathematical Methods of Classical Mechanics* (Springer, New York, 1989).

[48] L. Guo, V. Peano, M. Marthaler, and M. I. Dykman, Phys. Rev. A **87**, 062117 (2013).